Using Nanoporous Core-Samples to Mimic the Effect of Petrophysical Parameters on Natural Gas Flowrate in an Unconventional Gas Reservoir

Evans Ogoun, Ofasa Abunumah, Florence Aisueni, Mamdud Hossain, Ayo Giwa and Edward Gobina*

Centre for Process Integration and Membrane Technology,
School of Engineering, Robert Gordon University, Aberdeen, United Kingdom. AB10 7QB,
*Corresponding Author: E-mail: e.gobina@rgu.ac.uk; Phone: +44(0)1224262348
McAlpha Inc, Calgary, Canada, info@mcalpha.com

ABSTRACT

Natural gas was for quite a long time regarded as an unwanted by-product of oil exploration and production that was mostly flared to the atmosphere. This happened because there was no feasible economic means of bringing it to the market. In this work ceramic core technology, which has gained significant attention over the last decades, will be applied to enable laboratory study of the permeation of gases continuously under mild conditions and under realistic pressure drops with very low consumption of energy with no required additives. The study is designed to mimic the effect of petrophysical parameters on gas flow in a tight reservoir using nano-porous core samples. Experiments were carried out, involving a procedure that requires the release of different gases contained in a gas cylinder to an assemblage of nano-cores fitted into the centre of an anulus of a shell and tube arrangement. The nano-core samples had varying pore throats and were studied at different temperature and pressure conditions. Suitable data were collected and analysed with statistical tools to showcase the influence of petrophysical parameters on the flowrate associated in extracting gas from unconventional reservoirs. The results established that several factors impact on the accumulation and migration of gas in an unconventional gas reservoir and these factors determine the rate at which gas flows from the reservoir to the well-bore.

Keywords: Nanoporous, Petrophysical Parameters, Klinkenberg effect, non-Darcy flow.

INTRODUCTION

To effectively evaluate and quantify a typical reservoir in reservoir engineering applications a comprehensive insight of the reservoir petrophysical parameters are essential. These parameters include porosity, pore volume compressibility, permeability, relative-permeability, capillary-pressure, and liquid saturations (Abunumah et al 2021). For gas reservoir studies two main petrophysical features of interest are the Klinkenberg effect and non-Darcy flow (Bird et al 2002). Unconventional reservoirs have some characteristics properties that distinguishes its porous matrices from those of conventional reservoirs. The matrix permeability in these reservoirs is usually less than 0.1md (Kuuskraa 2004). According to investigation, tight reservoirs pores are classified as macropores (radius > 100m) and mesopores (radius 50-100m); fine throats (radius 1.0 – 2.0m), meso-throats (radius 2.0 - 4.0m), and coarse throats (radius > 4.0m) (Gao et al, 2019; Liu et al., 2021; Wu et al., 2018; Yu et al., 2020; Z. Zhang et al., 2016).

Klinkenberge Effect

Klinkenberg effect, also known as the slippage effect, is caused by low-pressure measurements because the pores in a reservoir rock are approximately the same with the mean free path of gas molecules, suggesting that the gas molecules are too widely apart to behave as a continuous fluid, resulting in a distorted high apparent permeability. The Klinkenberg effect enhances gas flow when pore sizes are very small and is important when permeability is lower than $10^{-18}m^2$ and at low pore pressure differentials, and its correction is necessary in estimating water permeability from measurement of gas permeability (Klinkenberg 1941).

Non-Darcy Flow

Darcy's law may not be precise to estimate reservoir parameters at high fluid velocities, a further energy loss is often apparent above that

predicted from Darcy's law of laminar flow. Non-darcy flow also known as turbulence flow arises due to multiple factors, such as pore scale as well as reservoir scale phenomena, and is commonly quantified through the Forchheimer equation. This is an empirical equation that links the pressure differential caused by friction in a porous medium to the velocity of the flow within the medium (javadpour and Difisher 2007)

MATERIALS AND METHOD

The experimental set and procedures used here are well established and have been used by other investigators such as (Abunumah et al., 2021; Ofasa Abunumah, Edward Gobina, et al., Ogunlude. et al. 2020). A rig was assembled with a porous ceramic core fitted into the centre of an annulus of a shell and tube mechanism and both ends covered with graphite seal to avoid gas leakage (Fig 1). A snoop solution is used to detect any leaks prior to each experiment. The analogues core samples used were selected such that they fall within the range of unconventional pore size profile mentioned in the literature (Gao et al., 2019). The experiment was conducted with 15nm and 200nm core samples and methane gas CH4 and carbon dioxide C02 which are components of natural gas were used. The system is heated to an assumed reservoir temperature 293K and allowed to reach thermal stability. Then, the gases were released and allowed to flow through the porous core at predetermined pressure intervals of 0.4bar to an exit line where the gas is discharge. The system is allowed to operate for a period until a steady state is achieved and the flow meter readings are stabilized. Once this stability is attained, the readings on the flow meter was recorded and other parameters evaluated (Table 1).

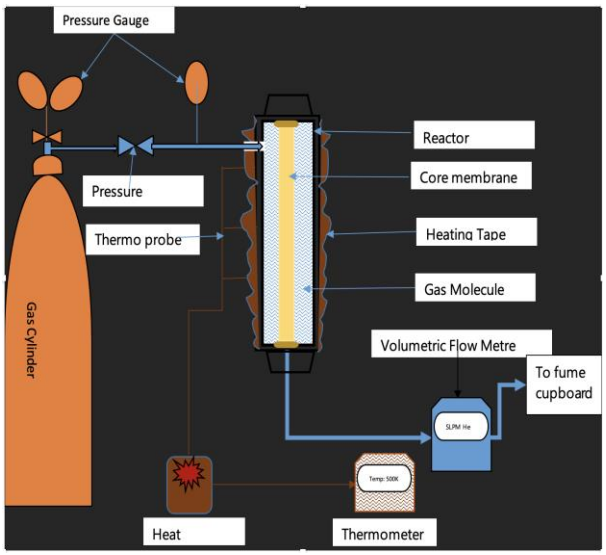

Fig 1: A Schematic of experimental set-up for gas permeation

RESULTS AND SUMMARY

The inverse average pressure was considered and plotted against the permeance (which is the measure of the degree to which the core sample allow gas to permeate) for the two different core samples and gases to demonstrate the Kinkenberg effect. According to Klinkenberg (1941), effective permeability at a finite pressure is given by

$$k_g = k_\infty(1 + b/p) \quad (1)$$

Where k_∞ is the absolute gas-phase permeability and b is the Klinkenberg factor dependent on the pore pressure of the region.
From the plot in figure 2, as the inverse average pressure increase the permeance tends to increase, and this is consistent with Klinkenberg equation on the assumption that average pore pressure is equivalent to pore pressure and permeability of water can be estimated from the slope of the plots.

In figure 3, the pressure drop was plotted against the flux to buttress the non-Darcy flow.
The Darcy formula for linear displacement is given by equation 2 (Whitaker, S., 1986).

$$q/A = Q = -\kappa\Delta P/\mu\delta \quad (2)$$

Where: q =fluid volumetric flowrate, m^3s^{-1}, A = cross-sectional area of the porous medium perpendicular to the flow, m^2, Q = fluid Volume flux, $m^3\ m^{-2}s^{-1}$ κ = absolute permeability, m^2, ΔP = pressure difference (Pa) across the distance parallel

to the direction of flow. μ = the fluid viscosity, Pa-s. δ = finite distance, m

The flux profile in fig 3 indicate a Darcy region and a non-Darcy region. A qualitative analysis of the graph indicates that the media and fluid properties affect the slopes of the Darcy region for each gas.
The flux Q was plotted against the pressure drop ΔP with the slop of the graph equals $-\kappa/\mu\delta$. The nature of the plots in fig 3 demonstrates that as pressure increase, the respective gases fluxes paths is observed to segregate further across and within the porous media, the segregation between the 15nm CH4 and 200nm CH4 and between 15nm CO2 and 200nm CO2 plots could be stated to be driven by pressure and porous media characteristics such as porosity, pore size and tortuosity. In this case increasing pore size from 15nm to 200nm causes a decrease in the flux of the two gases. Furthermore, the segregation between 15nm CH4 and 15nm CO2 is stated to be driven by pressure and fluid characteristic of the respective gases, such as molecular mass and viscosity. In this case, flux is inversely proportional to molecular mass. This flux-molecular mass relationship observed here fits well into Grahams law of diffusion (Knaff & Schlunder, 1985; Solcova et al., 2021) which states that the rate of effusion/diffusion is inversely related to the respective fluid molecular mass.

	A	B	C	D	E	F	G	H	I	J	K	L	M	N	O	P
1	CORE:15NM															
2									CH4				CO2			
3	Temperature (K)	Inlet pressure (Bar)	Outlet pressure (Bar)	Inlet pressure (Pa)	Outlet pressure (Pa)	Pressure drop (Pa)	Porosity (%)	Surface Area (M^2)	Flowrate (LPM)	Flowrate (M^3/S)	Flux (M^3/M^2S)	Permeance (M^3/M^2SPa)	Flowrate (LPM)	Flowrate (M^3/S)	Flux (M^3/M^2S)	Permeance (M^3/M^2SPa)
4	293	1.2	1	120000	100000	20000	13%	1.14	1.18	1.97E-05	1.73E-05	8.63E-10	0.87	1.5E-05	1.3E-05	6.3609E-10
5	293	1.6	1	160000	100000	60000	13%	1.14	2.29	3.8E-05	3.35E-05	5.58E-10	1.43	2.4E-05	2.1E-05	3.4851E-10
6	293	2	1	200000	100000	100000	13%	1.14	2.72	4.5E-05	3.98E-05	3.98E-10	1.68	2.8E-05	2.5E-05	2.4566E-10
7	293	2.4	1	240000	100000	140000	13%	1.14	2.97	5E-05	4.34E-05	3.10E-10	1.85	3.1E-05	2.7E-05	1.9323E-10
8	293	2.8	1	280000	100000	180000	13%	1.14	3.14	5.2E-05	4.59E-05	2.55E-10	1.96	3.3E-05	2.9E-05	1.5923E-10
9	293	3.2	1	320000	100000	220000	13%	1.14	3.27	5.5E-05	4.78E-05	2.17E-10	2.05	3.4E-05	3E-05	1.3626E-10
10	293	3.6	1	360000	100000	260000	13%	1.14	3.36	5.6E-05	4.91E-05	1.89E-10	2.11	3.5E-05	3.1E-05	1.1867E-10
11	293	4	1	400000	100000	300000	13%	1.14	3.43	5.7E-05	5.02E-05	1.67E-10	2.16	3.6E-05	3.2E-05	1.0528E-10
12																
13	CORE:200NM															
14									CH4				CO2			
15	Temperature (K)	Inlet pressure (Bar)	Outlet pressure (Bar)	Inlet pressure (Pa)	Outlet pressure (Pa)	Pressure drop (Pa)	Porosity (%)	Surface Area (M^2)	Flowrate (LPM)	Flowrate (M^3/S)	Flux (M^3/M^2S)	Permeance (M^3/M^2SPa)	Flowrate (LPM)	Flowrate (M^3/S)	Flux (M^3/M^2S)	Permeance (M^3/M^2SPa)
16	293	1.2	1	120000	100000	20000	20%	1.24	1.63	2.7E-05	2.2E-05	1.0956E-09	0.98	1.6E-05	1.3E-05	6.5873E-10
17	293	1.6	1	160000	100000	60000	20%	1.24	2.46	4.1E-05	3.3E-05	5.5119E-10	1.54	2.6E-05	2.1E-05	3.4505E-10
18	293	2	1	200000	100000	100000	20%	1.24	2.84	4.7E-05	3.8E-05	3.818E-10	1.79	3E-05	2.4E-05	2.4064E-10
19	293	2.4	1	240000	100000	140000	20%	1.24	3.07	5.1E-05	4.1E-05	2.948E-10	1.95	3.3E-05	2.6E-05	1.8725E-10
20	293	2.8	1	280000	100000	180000	20%	1.24	3.24	5.4E-05	4.4E-05	2.4198E-10	2.07	3.5E-05	2.8E-05	1.546E-10
21	293	3.2	1	320000	100000	220000	20%	1.24	3.36	5.6E-05	4.5E-05	2.0532E-10	2.14	3.6E-05	2.9E-05	1.3077E-10
22	293	3.6	1	360000	100000	260000	20%	1.24	3.45	5.8E-05	4.6E-05	1.7839E-10	2.2	3.7E-05	3E-05	1.1375E-10
23	293	4	1	400000	100000	300000	20%	1.24	3.53	5.9E-05	4.7E-05	1.5819E-10	2.26	3.8E-05	3E-05	1.0127E-10

Table 1: Summary of the experimental results and parameters

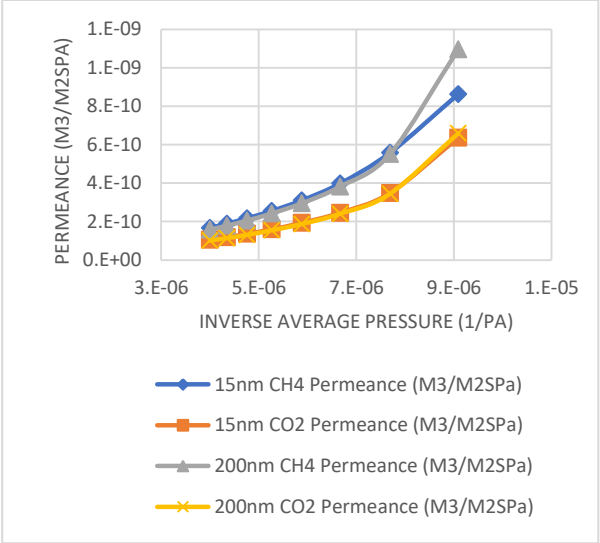

Fig 2: Effect of inverse average pressure on permeance for CH4 and CO2 for the two cores.

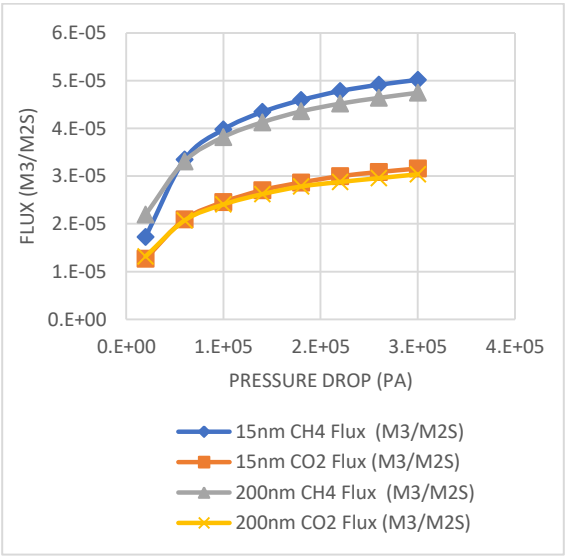

Fig 3: Effect of pressure drop on flux for CH4 and CO2 for the two cores.

CONCLUSION

The gas compressibility and pressure-dependent effective permeability distinguishes gas flow in porous media from liquid, this has significantly impacted on gas flow behaviour, especially in low permeability media thereby giving rise to the Klinkenberg effect and a deviation from the Darcy empirical model of simple linear relationship between flowrate and pressure drop. The experimental results indicate that Klinkenberg effect are significant in any

situation where the mean free path of gas molecules in porous media approaches the core diameter. From results, it can be found that many factors affect the permeability of gas flowing through nano pores, such as the gas mole weight, temperature, pressure, pore size, and gas viscosity. In addition, when reservoir temperature is increased and pore pressure is decreased, the contribution of slip effect and Knudsen diffusion to permeability will increase. More slip flow will be expected in the reservoirs at the condition of high temperatures and low pressures and this is due to the slip effect.

REFERENCE

Abunumah, O., Ogunlude, P., & Gobina, E. (2021). Experimental Evaluation of the Mobility Profile of Enhanced Oil Recovery Gases. Advances in Chemical Engineering and Science, 11(02), 154–164. https://doi.org/10.4236/ACES.2021.112010

Bird R.B., Steward W.E., and Lightfoot E.N. (2002) transport phenomena. 2nd edn. New York, USA. John Wiley & sons Inc 2002.

Gao, Y., Wang, Z., She, Y., Lin, S., Lin, M., & Zhang, C. (2019). Mineral characteristic of rocks and its impact on the reservoir quality of He 8 tight sandstone of Tianhuan area, Ordos Basin, China. Journal of Natural Gas Geoscience, 4(4), 205–214. https://doi.org/10.1016/J.JNGGS.2019.07.001

Javadpour F. and Difisher M. (2007) nano-scale gas flow in shale sediment. Journal of Canadian petroleum technology (46) pp 55-61

Klinkenberg, L. J. (1941) The permeability of Porous media to liquids and gases, American Petroleum Institute, Drilling and Productions Practices, 200–213. 1-23

Kuuskraa, V. A. (2004). Natural Gas Resources, Unconventional. Encyclopedia of Energy, 257–272. https://doi.org/10.1016/B0-12-176480-X/00279-5

Liu, Y., Zhang, X., Shi, J., Guo, W., Kang, L., Yu, R., Sun, Y., Wang, Z., & Pan, M. (2021). A reservoir quality evaluation approach for tight sandstone reservoirs based on the gray correlation algorithm: A case study of the Chang 6 layer in the W area of the as oilfield, Ordos Basin. Energy Exploration and Exploitation, 39(4), 1027–1056. https://doi.org/10.1177/0144598721998510

Ofasa Abunumah, Edward Gobina, & Priscilla Ogunlude. (2021). Experimental Validation of the Well Density Profile in Immiscible Gas Enhanced Oil Recovery Projects. J Chem Eng Process Technol, Vol. 12 Iss. 9. https://www.longdom.org/open-access/experimental-validation-of-the-well-density-profile-in-immiscible-gas-enhanced-oil-recovery-projects.pdf

Ogunlude, P., Abunumah, O., Orakwe, I., Shehu, H., Muhammad-Sukki, F., & Gobina, E. (2020). Upgrading biogas to biomethane by use of nano-structured ceramic membranes. Detritus, 12. https://doi.org/10.31025/2611-4135/2020.13996

Šolcová, O., Šnajdaufová, H., & Schneider, P. (2001). Multicomponent counter-current gas diffusion in porous solids: The Graham's-law diffusion cell. Chemical Engineering Science, 56(17), 5231–5237. https://doi.org/10.1016/S0009-2509(01)00149-X

Whitaker, S., 1986. Flow in porous media I: A theoretical derivation of Darcy's law. Transport in Porous Media.1: 3–25.

Wu, H., Ji, Y., Liu, R., Zhang, C., & Chen, S. (2018). Pore structure and fractal characteristics of a tight gas sandstone: A case study of Sulige area in the Ordos Basin, China: Https://Doi.Org/10.1177/0144598718764750, 36(6), 1438–1460. https://doi.org/10.1177/0144598718764750

Yu, C., Gong, D., Huang, S., Liao, F., & Sun, Q. (2014). Characteristics of light hydrocarbons of tight gases and its application in the Sulige gas field, Ordos basin, China. Energy Exploration and Exploitation, 32(1), 211–226. https://doi.org/10.1260/0144-5987.32.1.211

Zhang, W., Shi, Z., & Tian, Y. (2020). An improved method to characterize the pore-throat structures in tight sandstone reservoirs: Combined high-pressure and rate-controlled mercury injection techniques. Energy Exploration and Exploitation, 38(6), 2389–2412. https://doi.org/10.1177/0144598720920729

Zhang, Z., Shi, Y., Li, H., & Jin, W. (2016). Experimental study on the pore structure characteristics of tight sandstone reservoirs in Upper Triassic Ordos Basin China. Energy Exploration and Exploitation, 34(3), 418–439. https://doi.org/10.1177/0144598716631667